

# Multigrid Acceleration of a Relaxation Procedure for the Reduced Navier-Stokes Equations

A. Himansu\* and S. G. Rubin†  
University of Cincinnati, Cincinnati, Ohio

The multigrid method is applied to obtain significant improvements in the convergence rate of an iterative relaxation procedure for the numerical solution of the reduced Navier-Stokes equations. The iterative algorithm uses "streamwise" marching sweeps, in a line-relaxation mode, to determine the pressure field. With the use of the multigrid procedure, considerable computational work multiplied by memory efficiency results for both inviscid transonic flow and laminar viscous flow with strong interaction. In addition to applying the standard Full Approximation Storage multigrid technique (full coarsening), a modified technique involving multigridging in only the streamwise direction (semicoarsening) is investigated. The latter is shown to be significantly better for flow behavior that is sensitive to grid stretching in the direction normal to the body surface. The problems considered in this study include trailing-edge flow (where the pressure gradient is singular), separated flow in a Carter-Wornom trough, and transonic inviscid flow over a parabolic-arc airfoil.

## Introduction

NUMERICAL solutions to the full Navier-Stokes (NS) equations usually require considerable computer memory and computational speed for the fluid-flow problems that are of current interest. In recent years, it has been shown by Rubin and coworkers that, for a large class of flow problems, the full NS equations can be approximated with negligible loss in accuracy by the reduced Navier-Stokes (RNS) system, in which selected viscous terms are omitted. The primary advantage of the RNS approximation is improved computational efficiency, i.e., fewer iterations and less storage. By using an appropriate coordinate system, flows involving strong viscous-inviscid interaction, axial-flow separation, shock interactions, and upstream influence can be determined from the RNS model. The ellipticity of the equations is represented by an inviscid (acoustic) pressure interaction rather than by axial viscous diffusion. This is reflected in the formulation of an unconditionally stable line-relaxation solution procedure for the RNS equations, presented in an earlier study by Rubin and Reddy.<sup>11</sup> This iterative procedure uses marching sweeps, from inflow to outflow, to decrease the error of a stored pressure field. The velocities are generated during each sweep; storage of the velocities is necessary only in regions of separated flow, if upwind differencing is used for the streamwise convective terms. This algorithm has been applied to the computation of several incompressible and subsonic/transonic steady flows with strong interaction and/or upstream influence by Reddy and Rubin<sup>10,11</sup> Khosla and Lai<sup>5,6</sup> and Ramakrishnan and Rubin.<sup>8</sup>

It has been shown by Rubin and coworkers that, for very small streamwise step-size and large subsonic extent of the computational domain in the "normal" direction, the convergence of the relaxation procedure slows markedly. In the present study, this difficulty is addressed and overcome by the use of a multigrid method to accelerate the convergence of the

algorithm. The multigrid method employs a hierarchy of grids and speeds up transfer of information across the flow domain by solving related problems on coarser grids, while maintaining fine-grid accuracy. Recently, Israeli and Rosenfeld<sup>4</sup> have demonstrated some success in the application of the multigrid technique to RNS line relaxation. They introduce a source term that improves the error-smoothing properties of the line-relaxation procedure. The present study explores the importance and effects of this source term.

Large Reynolds number flow solutions are typically sensitive to grid stretching and distribution in the direction normal to the surface; therefore, the solutions may not be well represented on the coarser grids required in the multigrid method. For this reason, a modified technique that uses the multigrid philosophy in only the streamwise direction is also investigated in the present study. Comparisons between full coarsening and semicoarsening approaches reflect the strong influence of grid stretching on the multigrid strategy and the importance of semicoarsening for the class of problems considered herein.

## Governing Equations

For the flow problems considered in the present study, it is possible to use the condition of constant stagnation enthalpy in lieu of the full differential energy equation. With this simplification, the RNS equations for steady, two-dimensional, laminar, compressible flow, written in conservative form and in a sheared Cartesian coordinate system  $(\xi, \eta)$ , are given as follows:

Continuity:

$$(\rho u)_{\xi} + (\rho v)_{\eta} = 0 \quad (1)$$

x momentum:

$$(\rho u^2)_{\xi} + y'_b (\rho uv + y'_b \rho u^2)_{\xi} + [(1 + y'^2_b) \rho uv + y'_b \rho v^2]_{\eta} + p_{\xi} - \frac{1}{R} (\mu u_{\eta})_{\eta} = 0 \quad (2)$$

y momentum:

$$(\rho uv + y'_b \rho u^2)_{\xi} + (\rho v^2 + y'_b \rho uv)_{\eta} + p_{\eta} = 0 \quad (3)$$

Presented as Paper 87-1145 at the AIAA 8th Computational Fluid Dynamics Conference, Honolulu, HI, June 9-11, 1987; received Aug. 27, 1987; revision received Feb. 28, 1988. Copyright © American Institute of Aeronautics and Astronautics, Inc., 1987. All rights reserved.

\*Graduate Research Assistant, Aerospace Engineering. Student Member AIAA.

†Head and Professor, Aerospace Engineering. Associate Fellow AIAA.

Constant stagnation enthalpy:

$$T + \frac{(\gamma - 1)}{2} M_\infty^2 [u^2 + (v + y'_b u)^2] = \text{const} = H_\infty \quad (4)$$

Equation of state:

$$p = \frac{\rho T}{\gamma M_\infty^2} \quad (5)$$

Viscosity law:

$$\mu = T^w \quad (6)$$

Equations (1-6) are given in dimensionless, primitive variable form. The freestream Mach number is  $M_\infty$  and  $R$  is the Reynolds number based on freestream conditions and some reference length. A shearing transformation is used to simplify the application of the boundary conditions; the transformation from Cartesian  $(x, y)$  to sheared coordinates  $(\xi, \eta)$  is given by

$$\xi = x; \quad \eta = y - y_b(x) \quad (7)$$

The Cartesian normal or  $y$  component of velocity  $V$  is related to the transformed velocity  $v$  by

$$v = V - y'_b u \quad (8)$$

In Eqs. (7) and (8),  $y_b(x)$  defines the body surface, and  $y'_b$  defines the slope of the surface.

Inflow boundary conditions are specified on  $u$ ,  $v$ ,  $\rho$ , and  $p$ , and an outflow boundary condition is required only for  $p$ . In the  $\eta$  direction, one boundary condition is required for each of  $v$  and  $\rho$ , and two for  $u$ . The RNS approximation, equations, and boundary conditions are discussed more completely in Refs. 5-11 and in the section on results in this paper.

### Numerical Discretization and Relaxation Scheme

The RNS equations contain all the terms in the Euler as well as the interacting boundary-layer and triple-deck equations. The mechanism that provides acoustic or upstream influence is the coupling between the streamwise pressure-gradient term in the "axial" momentum equation and the axial convection term in the "normal" momentum equation. Axial-flow diffusion as well as all diffusion terms in the normal momentum equation [Eq. (3)] are negligible; therefore, the RNS equations contain only convective and pressure axial-flow derivatives. These are of first order with respect to the streamwise coordinate  $\xi$ . If these terms are discretized with backward differences, as for an initial-value problem, solutions can, in principle, be obtained by marching in the streamwise direction with prescribed initial conditions. However, it was shown by Vigneron et al.<sup>14</sup> that, for well-posedness of the initial-value problem, only a portion ( $\omega p_\xi$ ) of the pressure-gradient term can be treated implicitly. The factor  $\omega$  is given by  $\omega = \alpha \omega_M$ , where  $0 \leq \alpha \leq 1$  and

$$\omega_M = \min[f(M_\xi), 1] \quad (9a)$$

$$f(M_\xi) = \gamma M_\xi^2 / [1 + (\gamma - 1) M_\xi^2] \quad (9b)$$

where  $M_\xi$  is the Mach number of the streamwise velocity component.

The correct form of the pressure-gradient discretization has been obtained in Refs. 5-11 by incorporating the elliptic or boundary-value nature of the problem in subsonic flow regions. The pressure-gradient term is written as

$$\omega(p_\xi)_h + (1 - \omega)(p_\xi)_e$$

where  $(p_\xi)_h$  is the "hyperbolic" portion of the pressure gradient, which is backward-differenced;  $(p_\xi)_e$  is the "elliptic"

portion of the pressure gradient, which is forward-differenced to allow for upstream influences. It can be seen from Eq. (9) that  $p_\xi$  is almost fully forward-differenced in low subsonic regions and almost fully backward-differenced in high-subsonic or supersonic regions. In particular, for incompressible flow,  $p_\xi$  is only forward-differenced; the interpretation of this differencing is discussed with reference to a staggered grid, in earlier studies. The  $\xi$  derivatives of the convective terms are backward-differenced to first- or second-order accuracy. This follows the characteristic domain of dependence and physical mechanism of flow convection.

The continuity equation is discretized about  $(i, j - 1/2)$ , the  $x$ -momentum equation about  $(i, j)$  and the  $y$  momentum equation about  $(i, j + 1/2)$ . All  $\eta$  derivatives are second-order accurate.

The discretized system leads to a set of coupled nonlinear equations for  $u$ ,  $v$ ,  $\rho$ , and  $p$ . The solution operator  $S^h$  applied here is of the iterative line-relaxation type. The equations are written at a given streamwise station ( $\xi = \text{const}$  line, indexed by  $i$ ) and are solved to a prescribed level of accuracy before proceeding to the next downstream station. The quantities having the index  $(i)$  represent the unknowns at the station  $i$ . The pressure  $p_i$  is eliminated from the momentum equations, in favor of the density and the velocities, with the aid of the constant stagnation enthalpy condition [Eq. (4)] and the equation of state [Eq. (5)]. The nonlinear terms are quasilinearized to second order about the previous local iterate or guessed value. The resulting linear system is inverted by a standard LU decomposition. The computed unknowns are used to update the previous iterate, and the inversion is repeated until local convergence is achieved. At any station  $i$ , the downstream pressure  $p_{i+1}$  appearing in the equations is unknown. This leads to a global iteration process. The equations are marched downstream, with  $p_{i+1}$  prescribed from the previous global iteration. The pressure is then updated by the computation at  $i+1$ . This process is repeated until convergence is achieved, i.e., the change in the pressure field from iteration to iteration is reduced to a prescribed tolerance. For unseparated flows, the algorithm requires storage of the pressure field only; the velocities are generated during each marching sweep. It should be noted here that numerical information from the flow at any downstream location propagates upstream only one mesh width per global iteration. This is typical of line-relaxation smoothers.

The stability and convergence properties of the global-relaxation procedure have been investigated by Reddy and Rubin.<sup>10</sup> Their analysis shows that the asymptotic convergence factor or spectral radius of the global iteration procedure is  $1 - O[(\Delta\xi/\eta_M)^2]$ , where  $\eta_M$  is the normal extent of the subsonic flow region. This shows that, for very fine meshes in the  $\xi$  direction and/or large  $\eta_M$  (both of which are frequently necessary to resolve flows with strong iteration), the convergence process slows significantly.

At this point, it is seen that there is a threefold advantage to a multigrid method to improve the convergence rate of the global relaxation procedure: 1) one iteration on a coarser grid costs less computer time than one on the fine grid because fewer grid points are involved; 2) with fewer streamwise stations (larger mesh width) on the coarse grid, information from downstream reaches the inflow in a reduced number of global iterations; 3)  $\Delta\xi/\eta_M$  is larger for the coarse grid, and therefore the iteration on the coarse grid has a lower convergence factor.

Israeli and Lin<sup>3</sup> have proposed a modification of the streamwise pressure-gradient term in the global pressure-relaxation algorithm to improve the stability of the smoothing or relaxation operator. It takes the form of a pressure source term (hereafter referred to as the Israeli source term or IST), that vanishes on convergence. For  $\omega = 0$ , the  $x$ -momentum equation can symbolically be written as

$$p_{i+1}^n - p_i^n = R_i + s_i^n \quad (10)$$

where  $R_i$  represents all nonpressure terms. The superscript  $n$

denotes pressure values being computed during the current global iteration, and  $n-1$  denotes the values from the previous global iteration. The IST  $s_i^n$  satisfies

$$s_i^n - s_{i-1}^n = p_i^n - p_{i-1}^{n-1} \quad (11)$$

The resulting relaxation process then possesses the improved error-smoothing properties of successive line relaxation. As discussed in the section on results, this is important for proper transfer in the multigrid process. For single-grid considerations, the IST can be either used in conjunction with over-relaxation or omitted altogether. Israeli and Rosenfeld<sup>4</sup> have applied multigrid acceleration successfully to RNS computations with the IST for the flow past a semi-infinite flat plate.

### Multigrid Method

The multigrid method is a technique to accelerate the iterative solution of boundary-value problems on continuous domains. In recent years, there has been a proliferation of papers in this field, and the method has been extended to solve problems other than partial differential equations on continuous domains. A fairly extensive bibliography of the multigrid literature may be found in Ref. 13.

The basic idea behind the multigrid method can be described briefly as follows. A general boundary-value problem on a continuous domain  $D$  is discretized on a grid of mesh size  $h$ . The discrete problem may be represented as

$$L^h u^h = f^h \quad (12)$$

where  $u^h$  is the (discrete) grid function being solved for,  $L^h$  is the discrete (finite-difference, finite-element, etc.) operator analog of the continuous partial-differential matrix operator, and  $f^h$  is a given function of the position vector.

Iterative methods begin with an initial approximation  $u_0^h$  to the exact solution  $u^h$  of Eq. (12) and involve the repeated application of an error-reducing operator or process  $S^h$  (usually a "relaxation" operator, such as the Gauss-Seidel or Jacobi pointwise relaxation schemes) to generate a sequence of iterates  $u_n^h$  of the grid function. In the present scheme, the process consists of streamwise marching sweeps. At any iteration level  $n$  denote the error grid function by

$$v_n^h = u^h - u_n^h \quad (13)$$

The residual or defect of  $u_n^h$  is defined by

$$r_n^h = f^h - L^h u_n^h \quad (14)$$

The residual is a grid function similar to the error, but it carries information about how much  $u_n^h$  fails to satisfy Eq. (12). In the present scheme, the continuity and  $y$ -momentum equations are solved exactly and their residuals are zero. Only the residual associated with the  $x$ -momentum equation is nonzero; this is due to the updating of pressure at the  $i+1$  location.

It is characteristic of many processes of  $S^h$  for discrete systems originating in continuous problems that they relax the equations in Eq. (12) locally. More precisely, they produce a smooth (i.e., slowly varying) residual grid function. Repeated application of the operator  $S^h$  will have greatly reduced the small-wavelength or nonsmooth Fourier components of the error but will have had less effect on the large-wavelength or smooth components. It is then that the operator  $S^h$  tends to its asymptotic convergence rate; this is often extremely slow, since the local nature of the relaxation  $S^h$  is ineffective on long-range errors.

Using Eq. (12), Eq. (14) may be rewritten as

$$L^h u^h - L^h u_n^h = r_n^h \quad (15)$$

which is seen to be equivalent to Eq. (12).

In the multigrid method, Eq. (15) is now transferred to a coarser grid with mesh size  $H$ . In standard full coarsening,  $H=2h$  and every other grid line of the grid  $h$  is selected to form the grid  $H$ . Equation (15) is replaced by a coarse-grid analog:

$$L^H \bar{u}^H - L^H u_n^H = r_n^H \quad (16)$$

where  $u_n^H$  and  $r_n^H$  are known from the  $n$ th iteration on the fine grid, and  $\bar{u}^H$ , which is governed by Eq. (16), may be regarded as a coarse-grid representation of  $u^h$ .

It is noted that, if  $r_n^h$  is smooth, it can be well represented on the coarse grid  $H$ . By transferring the second term in Eq. (16) to the right-hand side, it is seen that Eq. (16) is of the form of Eq. (12) and, hence, can be solved on grid  $H$  using the analog  $S^H$  of  $S^h$ . Solving Eq. (16) requires less work than solving Eq. (15) because, first, for a two-dimensional domain, Eq. (16) would involve only one-fourth as many unknowns as Eq. (15). Second, due to the larger mesh size  $H$ , information travels faster from region to region of the grid and results in an improved convergence rate. From Eq. (15), we may postulate that, if  $r_n^h$  is smooth enough, for most operators  $L^h$  the error function will also be smooth. Once Eq. (16) has been solved to a prescribed degree of accuracy,  $u_n^H$  is interpolated back to grid  $h$  to obtain a good approximation to  $v_n^h$ ; thus, the major work in solving Eq. (15) has been carried out less expensively on a coarser grid  $H$ . We note here that no requirement is made that  $f^h$  and  $u^h$  be smooth.

If the grid  $H$  is itself extensive enough to make solving Eq. (16) expensive, Eq. (16) is smoothed (relative to grid  $H$ ) by application of  $S^H$  and is then transferred to a still coarser grid, in the same way Eq. (16) was obtained from Eq. (15). In fact, if the transferred problem to be solved on any grid is not converging fast enough, it is transferred to a coarser grid to improve convergence.

### Multigrid Components

From the previous paragraphs, it is seen that there are three basic operations involved in the "coarse-grid correction" cycle: the relaxation  $S^h$  or  $S^H$ , a transfer of  $r_n^h$  and  $u_n^h$  from the fine to the coarse grid (often termed a "restriction"), and an interpolation of the error from the coarse to the fine grid (termed a "prolongation").

Relaxation:

$$u_n^h = S^h u_{n-1}^h$$

On any grid, the role of the smoother  $S^h$  is to efficiently reduce the small-wavelength errors. The large-wavelength error components will be reduced on coarser grids, relative to which they appear as small-wavelength components.

Restriction: Equation (16), which is to be solved on the coarse grid, may be written with all the known quantities on the right-hand side as

$$L^H \bar{u}^H = r_n^H + L^H u_n^H = I_H^H r_n^h + L^H \hat{I}_h^H u_n^h \quad (17)$$

Here  $I_H^H$  and  $\hat{I}_h^H$  are fine-to-coarse-grid transfer operators, which need not be the same. In the present study, the full-weighting operator, as recommended by Brandt,<sup>2</sup> was used for transfer of the  $x$ -momentum residual. The restriction of  $u_n^h$  was taken to be the simple injection operator.

Prolongation:

$$u_{n+1}^h = u_n^h + I_h^H (\bar{u}^H - \hat{I}_h^H u_n^h) \quad (18)$$

where  $I_h^H$  is the prolongation or coarse-to-fine-grid interpolation operator for the coarse-grid representation of the error function. It may be noted that it is the error  $(\bar{u}^H - \hat{I}_h^H u_n^h)$  that must be interpolated and not  $\bar{u}^H$ , for it is the error that is smooth;  $u^h$  may be nonsmooth so that the direct interpolation of  $\bar{u}^H$  may introduce large nonsmooth errors on the fine grid.

In the present study, only the pressure field is stored and, hence, only the pressure error function is interpolated back to the fine grid. Bilinear interpolation was used for this error function.

#### Convergence and Work Measures

The multigrid method uses a hierarchy of successively finer grids indexed by  $1, 2, \dots, k, \dots, M$ . The unit of work is defined as the work required to perform one relaxation sweep on the finest grid  $M$ . If full standard coarsening is used for a two-dimensional problem, neglecting boundary effects, the work of one relaxation sweep on grid  $k$  is taken to be  $(1/4)^{(M-k)}$  work units. The work involved in computing the residual and effecting the intergrid transfers has been neglected in comparison to that for the relaxation steps.

Since the flow problems that have been solved in this study are well conditioned, the solution quality at any iteration level has been measured by a residual norm instead of an error norm. The norm used is the usual  $L_2$  norm (rms value).

We must note here that, when a problem is transferred from a grid  $k$  to a coarser grid  $k-1$ , it does not pay to solve the coarser-grid problem exactly. At most, one should bring the coarse-grid error down to the level of the nonsmooth error that will be introduced on the fine grid by the prolongation operator. In the present study, the accommodative  $C$  cycle has been used (see Ref. 1). In this cycle, if the convergence on any grid  $k$  is too slow, the problem is transferred to the coarser grid  $k-1$  where it is solved to a level where the coarse-grid residual norm is some fraction of the norm on the grid  $k$  when the problem was transferred.

#### Semicoarsening

In certain boundary-value problems, for example, fluid-flow problems with thin, strongly perturbed boundary layers, the discrete solution may be extremely sensitive to the mesh size and stretching in one coordinate direction; for boundary layers with strong viscous-inviscid interaction, this is typically the coordinate normal to the wall. In such cases, the standard full-coarsening procedure may not work very well because the fine-grid problem cannot be well represented on the coarse grid. This has been the experience of all previous multigrid investigators. One solution to such a difficulty is to eliminate the grid coarsening in that direction and use the multigrid concept only in the others. For example, if the problem is sensitive to the grid spacing in the  $\eta$  direction, the coarse grid is formed by taking every  $\eta$ -const grid line and, as before, every other  $\xi$ =const gridline. This is termed semicoarsening.<sup>2,13</sup>

In the present RNS study, some of the problems considered have precisely this characteristic. Hence, the use of semicoarsening for these problems was investigated. The relaxation operator is implicit in the  $\eta$  direction, so that the coupling of the unknowns is good in this direction. Coarsening to speed up information transfer is less critical in this direction. The disadvantage of semicoarsening is that, in two dimensions, the next coarse grid has about half as many points as the fine grid. Therefore, a coarse-grid relaxation sweep would cost half a fine-grid work unit, instead of the one-fourth unit it would cost on a grid obtained by standard full coarsening. The work of one relaxation sweep on grid  $k$ , in the semicoarsening procedure, is taken to be  $(1/2)^{(M-k)}$  work units. The residual restriction and error prolongation operators used are one-dimensional versions of those in the full-coarsening procedure. The stronger convergence properties of the semicoarsening approach for highly stretched grids can outweigh the associated work penalty, as is discussed in the next section.

## Results

#### Trailing-Edge Flow

The first problem considered has been solved by Reddy and Rubin<sup>10</sup> using the global relaxation procedure. It was chosen

here because of the strong viscous-inviscid interaction and large pressure gradients. The incompressible laminar flow at zero incidence past a finite flat plate of unit length is considered; the Reynolds number is based on plate length. The geometry is simply  $y'_b = 0$ . The specific boundary conditions associated with this geometry are as follows:

No-slip, no-injection conditions at the wall:

$$u=0, \quad v=0 \quad \text{at} \quad \eta=0$$

Beyond the trailing edge, the no-slip and no-injection conditions are replaced by the symmetry conditions:

$$u_\eta=0, \quad v=0$$

Freestream conditions at the outer  $\eta$  boundary:

$$u=1, \quad p=0 \quad \text{at} \quad \eta=\eta_M$$

Outflow pressure boundary condition:

$$p_\xi=0 \quad \text{at} \quad \xi=\xi_M$$

It may be noted that the freestream and outflow boundary conditions can be applied at much smaller distances from the body than is possible with NS solvers. This is because the difference equations reflect the convective character of the flow and the acoustic propagation. Thus, the outflow boundary can be relatively close to the body. The velocities at the outflow are computed and do not need to be prescribed. For subsonic flow, the outflow needs to be only far enough away to ensure negligible acoustic propagation. For supersonic flows, no outflow condition is needed. Similarly, the two-point differencing of the continuity and  $y$ -momentum equations do not require the prescription of  $v$  at the freestream boundary. The upwind differencing yields solutions without the spatial oscillations associated with the central differencing of the convective terms often employed in full NS solvers.

To circumvent problems arising at the leading edge  $\xi=0$ , the inflow is set at  $\xi=\xi_i > 1$ . The inflow conditions  $u_{in}$  and  $v_{in}$  are prescribed from a boundary-layer computation.

The flow near the trailing edge assumes the triple-deck structure first elucidated by Stewartson.<sup>12</sup> The interaction region is characterized by a parameter  $\epsilon = Re^{-1/3}$ . The streamwise extent of the region is of  $O(\epsilon^3)$ . In the normal direction, three regions or decks may be distinguished. The lowest deck is viscous in nature and has a normal extent of  $O(\epsilon^5)$ . The middle deck is the displaced boundary layer and is an inviscid but rotational region with a thickness of  $O(\epsilon^4)$ . The upper deck is an inviscid, irrotational region with a thickness of  $O(\epsilon^3)$ . Rubin and Reddy have shown that the RNS equations contain all of the terms necessary to capture this behavior, if the mesh sizes chosen are fine enough to resolve the flow. The

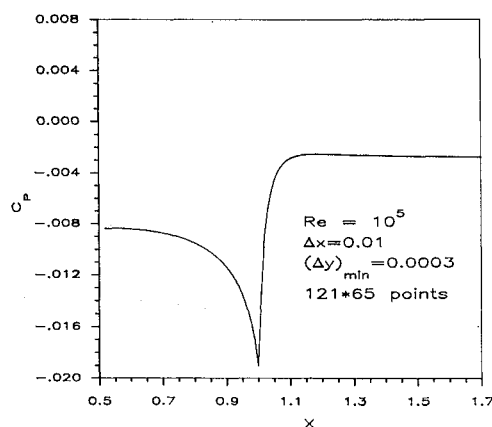


Fig. 1 Trailing-edge flow: coefficient of pressure.

computation is carried out from  $\xi=0.52$  to 1.72 and from  $\eta=0$  to  $\eta=0.6$ , for a Reynolds number of  $10^5$ . A uniform grid of  $\Delta\xi=0.01$  was used in the  $\xi$  direction. The value of  $\Delta\eta$  at the wall was 0.0003. Significant grid stretching was required in the  $\eta$  direction. A  $(121 \times 65)$  grid in the  $(\xi, \eta)$  directions was specified.

The solution for this case, with the same grid, has previously been obtained by Reddy and Rubin.<sup>10</sup> No comparison with other numerical or analytic data is given in this study, since the algorithm employed has already been validated earlier by Reddy<sup>9</sup> and Rubin and coworkers.<sup>10,11</sup> The primary focus of the present work has been the acceleration of the convergence of the algorithm. The pressure coefficient is shown in Fig. 1. It is in good agreement with the solution obtained by Reddy and Rubin.<sup>10</sup>

Attempts to use the multigrid method without the IST for this problem failed. The reason was that, although the relaxation exhibited good convergence properties, a nonsmooth residual function on the fine grid remained. This function is not well represented on the coarser grid; hence, the coarse-grid correction does not contribute significantly to reducing the fine-grid error. However, use of the IST produces a smooth residual function, although the solution itself is not smooth. The residuals at neighboring stations are of the same sign and nearly of the same magnitude. As a result, the fine-grid problem is very well represented on coarser grids, so that most of the solution is done on the coarsest grid. This results in good convergence of the multigrid (MG) algorithm. The MG convergence rate is shown in Fig. 2 for different grid levels. Semicoarsening has been applied throughout. It is seen that use of the multigrid method results in a considerable savings of computer time at the expense of a small increase in memory

requirement. An accurate MG solution is obtained in a hundred iterations. This contrasts with thousands of iterations to obtain a similar level of accuracy on a single grid.

In Fig. 3, a comparison of the performance of the full-coarsening and semicoarsening schemes is presented. In this case, it is seen that the semicoarsening is far superior. With the full-coarsening approximation, it is found that, as increasingly coarser grids are used, although the convergence on the coarsest grid is improved, the coarsest grid is unable to represent properly the variation of the solution in the normal direction. This effect appears as a drop in the residual norm when the problem is transferred from the finest to the coarsest grid (via the intermediate grids), and an upward jump in the norm when the error is interpolated back from the coarsest to the finer grids. The semicoarsening procedure is not affected by this problem. Therefore, it is a much more effective approach for flow problems in which the solution is very sensitive to the mesh distribution.

#### Carter-Wornom Trough

The multigrid algorithm also has been applied to the flow past the trough investigated by Carter and Wornom.<sup>15</sup> The body is a semi-infinite flat plate with a smooth dip. The surface is given by

$$y_b = -d \operatorname{sech}[4(x-x_0)]$$

Computations were carried out at  $Re=80,000$ , a Mach number of 0.1, and with a uniform grid spacing of  $\Delta\xi=0.0125$ . The computation was carried out from  $\xi=1.0$  to  $\xi=4.0$ , with  $x_0=2.5$ . The grid was again highly stretched in the  $\eta$  direction. At the wall,  $\Delta\eta$  was 0.0005. The boundary con-

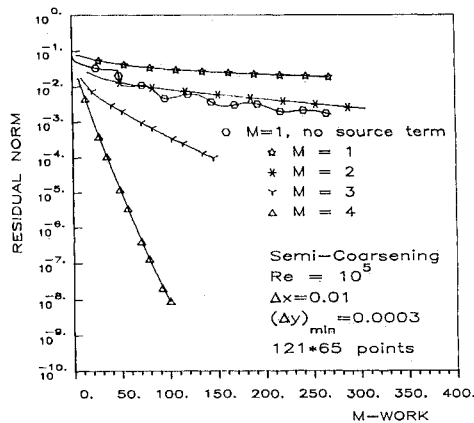


Fig. 2 Trailing-edge flow: MG convergence rate.

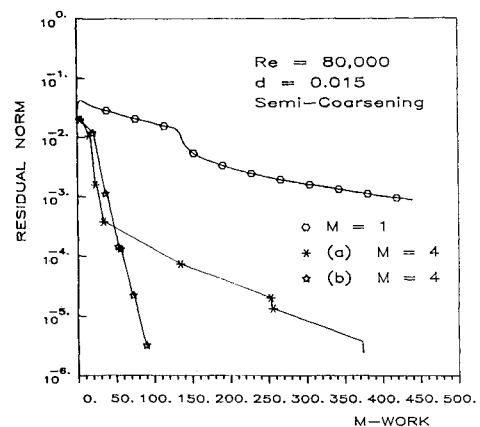


Fig. 4 Carter-Wornom trough: MG convergence rate.

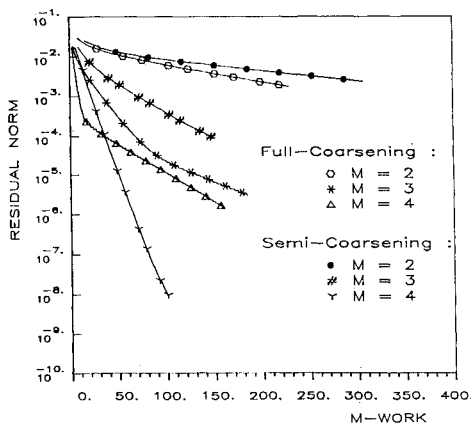


Fig. 3 Trailing-edge flow: comparison of full coarsening and semicoarsening.

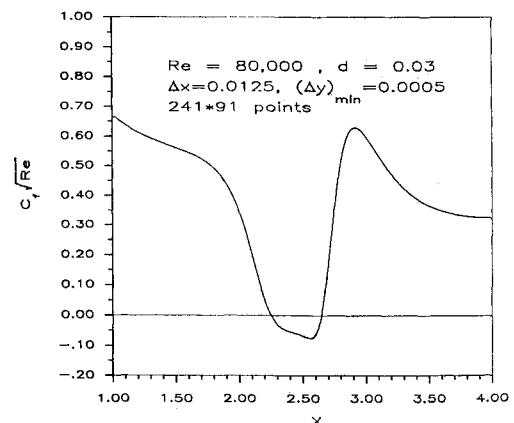


Fig. 5 Carter-Wornom trough: skin friction.

ditions are the same as for the flat-plate geometry; as discussed for the flat-plate problem, a boundary-layer profile is prescribed at the inflow.

Because of the fine mesh and large  $\eta$  extent of the domain, convergence on a single grid is extremely slow. The multigrid semicoarsening algorithm, with use of the IST, is seen in Fig. 4 to speed up the convergence rate significantly, for a trough of depth  $d=0.015$ . For the MG computations, the outer boundary was at  $\eta=3.0$ . However, the single grid (SG) relaxation without the IST displayed oscillatory convergence behavior. Therefore, the outer boundary was placed at  $\eta=15$  for the SG computation to obtain monotonic convergence. The curve labeled (a) was obtained with inclusion of the IST throughout the MG process. In the preliminary stages, it is seen that when the error level is high, the MG convergence rate is rapid. Later, the convergence process slows to the asymptotic convergence rate of the coarsest grid. Because of the IST, this is not much faster than that on the fine grid for relaxation without the IST. Two possible strategies to improve MG convergence rate are: 1) overrelaxation on the coarsest grid, in conjunction with the IST, and 2) relaxation without the IST on the coarsest grid. The latter strategy was employed, and the result is curve (b), which displays a satisfactory MG convergence rate even in the later stages. It was found necessary to introduce the IST during the last few iterations on the coarsest grid to smooth the error function before prolongation.

The trough problem was selected primarily to investigate multigrid performance in the presence of highly stretched grids and separated flows. For a trough of depth  $d=0.03$ , the boundary layer separates from the surface, and there is flow recirculation within the trough. Figures 5 and 6 show the skin-friction and pressure coefficients (based on twice the freestream dynamic pressure) for this case. The solution has

also been computed earlier by Reddy.<sup>9</sup> In the separated-flow region, the FLARE approximation was used in the  $x$ -momentum equation for these cases. This eliminates the further relaxation that would be introduced for the velocities in the separation region if upwind differencing were used. Figure 7 shows the significant improvement in convergence obtained by use of the semicoarsening multigrid procedure. This result represents an important step forward in the development of fast, low-storage algorithms for high Reynolds-number flows.

Full coarsening is, once again, ineffective for this separated-flow, highly stretched grid problem. The pressure field obtained on the fine grid by prolongation of the error function from the coarse grid caused divergence of the local iterations in the separated-flow region. Thus, the grid coarsening in the normal direction leads to a poor coarse-grid approximation to the error function.

A solution was next sought for a trough depth of  $d=0.06$  at a Reynolds number of 100,000. Curve (a) in Fig. 8 shows the skin-friction parameter for a step size of  $3/144$  in the  $\xi$  direction. Noteworthy is the "dip" in the curve before reattachment. The semicoarsening multigrid algorithm performed as expected. However, of greater interest in this case was the steepening of the dip and the appearance of oscillations on refining the fine-grid mesh size to  $3/200$ , as seen from curve (b) in Fig. 8. On further refinement, no converged solution was obtainable. The observation of a similar phenomenon in Navier-Stokes calculations with a direct solver for the laminar separation on a sine-wave airfoil by Bender and Khosla<sup>16</sup> at the University of Cincinnati, and asymptotic analysis by F.T. Smith and coworkers, both point to the result representing physical behavior rather than a numerical instability. It is hypothesized that the breakdown may represent the transition to turbulence, and further study in the form of the introduc-

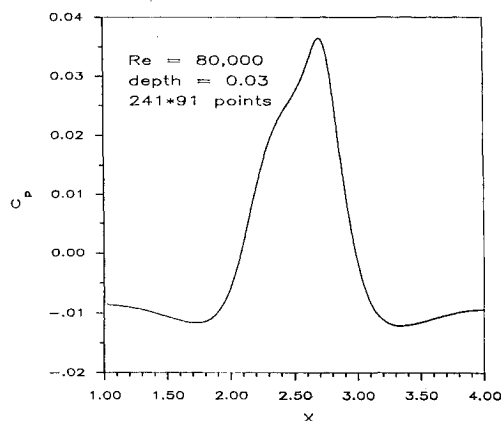


Fig. 6 Carter-Wornom trough: coefficient of pressure.

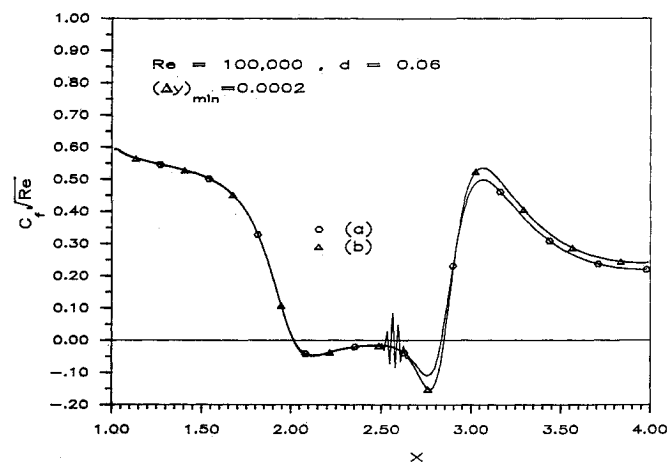


Fig. 8 Carter-Wornom trough: skin friction.

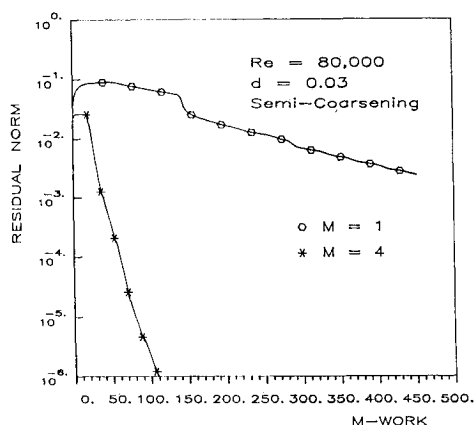


Fig. 7 Carter-Wornom trough: MG convergence rate.

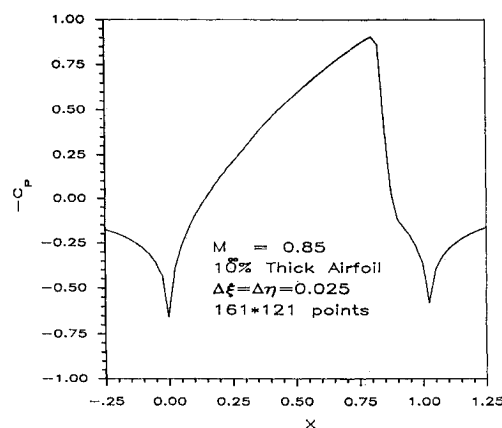


Fig. 9 Parabolic-arc airfoil: coefficient of pressure.

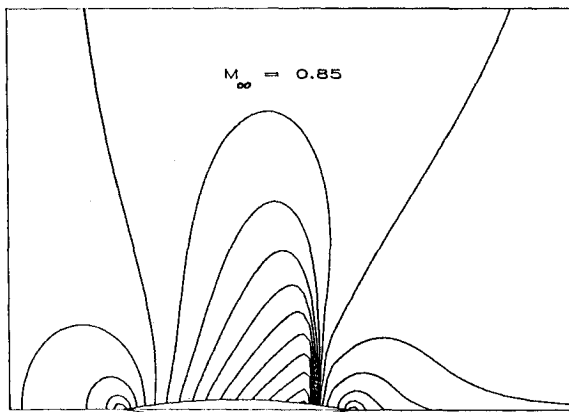


Fig. 10 Parabolic-arc airfoil: isomach contours.

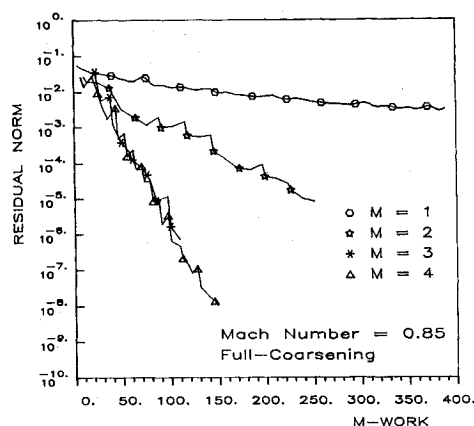


Fig. 11 Parabolic-arc airfoil: MG convergence rate.

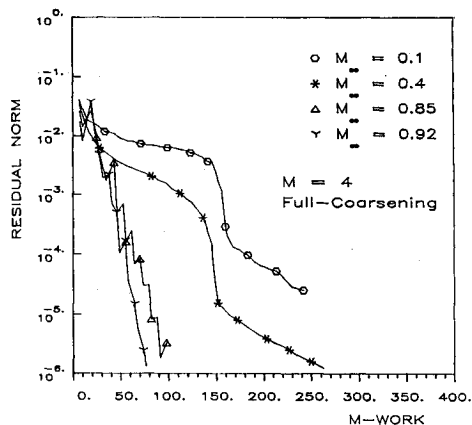


Fig. 12 Parabolic-arc airfoil: dependence of MG convergence rate on Mach number.

tion of a turbulence model in the separation region is under way.

#### Inviscid Transonic Flow Past a Parabolic-Arc Airfoil

Lai<sup>7</sup> has shown that the pressure-gradient splitting discussed in the section on numerical discretization is exactly that suggested by the characteristic analysis of the compressible Euler equations, and that the relaxation procedure should therefore be valid for the solution of inviscid flows as well. Lai has solved both the viscous and inviscid transonic flows past a parabolic-arc airfoil at zero incidence. The inviscid flow problem is used in the present study to test the performance of the multigrid method when discontinuities (shocks) are present in

the solution. The body surface of a parabolic-arc airfoil of unit chord is given by

$$y_b = 2tx(1-x)$$

where  $t$  is the chord-normalized maximum thickness of the airfoil.

The flow past a 10%-thick ( $t=0.1$ ) airfoil was computed for several Mach numbers. Uniform grid spacing of 0.025 was used for both coordinate directions. The grid of  $161 \times 121$  points extends from one chord upstream to two chords downstream and extends three chords in the  $y$  direction.

Uniform freestream conditions are specified at the inflow. For the inviscid flow,  $p=p_\infty$  is specified as the single outflow pressure boundary condition. Freestream conditions are imposed on  $u$  and  $\rho$  at the outer  $\eta$  boundary. On examining the definition of  $v$ , it is seen that  $v=0$  is a uniformly valid condition at  $\eta=0$ , both off (symmetry condition) and on (tangency condition) the body. Since inviscid flow ( $R=\infty$ ) is being computed, the viscous term in the  $x$ -momentum equation and the no-slip condition on  $u$  no longer appear. However, central differencing for the convective  $\eta$  derivatives in the  $x$ -momentum equation was retained; therefore, a continuation boundary condition is required. This is satisfied by the  $x$ -momentum equation written at the surface  $\eta=0$  ( $j=1$ ).

Figure 9 and 10 depict the pressure coefficient and isomach contours, respectively, for the flow at a freestream Mach number of 0.85. There is a shock in the region 0.825 to 0.875 on the airfoil surface. The body-slope discontinuities at the leading and trailing edges produce pressure peaks. The solutions shown here agree exactly with results obtained by Lai on a single grid.

The value of  $\alpha$  used in calculating the pressure-gradient splitting factor  $\omega$  was taken to be 0.96, except in the case  $M_\infty=0.92$ , when it was taken to be 0.93. Lower values of  $\alpha$  improve the convergence rate at the expense of increased numerical viscosity and smearing of the shocks. It is found that the SG convergence rate deteriorates somewhat with increasing Mach number.

In view of the better convergence properties and adequate smoothing properties of the relaxation without the IST, for compressible inviscid flow, the IST was not used for the parabolic-arc airfoil computations. Figure 11 shows the improvement in convergence rate by using the multigrid method with different numbers of grids. The freestream Mach number is 0.85, and a shock is present on the airfoil. Full coarsening was used for the cases shown. It is seen that there is a significant improvement in convergence rate, although the relaxation algorithm was used without the IST. Uniform grids were used in all cases. The rather jerky MG convergence is due to the error introduced in the interpolation from the coarse to the fine grid in the vicinity of the leading and trailing edges and the shock; this error causes a sharp rise in the residual on the fine grid, but this is quickly smoothed. The net effect of the coarse-grid relaxation is to improve greatly the convergence rate on the fine grid. In contrast to the viscous flow problems discussed previously, a significant number of iterations are required on the finest grid to counteract the error introduced by the prolongation and, thus, maintain the gain in convergence produced by the coarser grids.

Figure 12 displays the effect of freestream Mach number on the MG convergence rate. Full coarsening and four grids were used in all cases. Paradoxically, the MG performance improves with increasing Mach number. This is in sharp contrast to the SG case. This may be related to the splitting of the pressure-gradient term; the factor  $\omega$  increases with the Mach number; therefore, the pressure gradient more closely approximates an initial-value-type marching procedure.

The solution does not depend strongly on the grid in the normal direction. Hence, both full-coarsening and semicoarsening procedures were equally effective, with the former being more work-efficient than the latter. However, if

transonic viscous flow over the airfoil were being computed, one might speculate that the semicoarsening procedure would once again prove to be the more effective algorithm.

### Summary

The multigrid technique has been applied successfully to develop a storage-time efficient line-relaxation algorithm for the RNS equations. The results obtained clearly indicate the potential of multigrid methods for the fast numerical solution of the RNS system for viscous-inviscid low- and high-speed fluid-flow problems.

Storage for three residual fields and the pressure is required on the coarse grids. With four grid levels and full coarsening, overall storage is approximately 2.3125 times the storage required for pressure on the finest grid. The increase in storage is much less than for the full Navier-Stokes equations (these require overall storage of approximately 4.969 times that for the fine-grid pressure). With the significant improvement in multigrid convergence, the overall (work  $\times$  storage) efficiency is enhanced greatly.

Convergence rate studies of the algorithm have been made for the steady incompressible laminar flow past the trailing edge of a finite flat plate. The multigrid convergence was much faster than the single-grid convergence. The success of the multigrid process was found to depend strongly on the efficiency of the underlying relaxation method as an error smoother. The computed structure of the small viscous-inviscid interaction region at the trailing edge is sensitive to the grid spacing and stretching in the normal direction. Flow-property variations in the normal direction cannot be well represented on coarser grids. In this instance, it was found that the performance of the standard multigrid procedure was hindered by this circumstance. A semicoarsening version of the multigrid method, where the grid spacing in the normal direction was the same on all grids, was implemented. This resulted in greater computational efficiency. In the case of separated flow in a Carter-Wornom trough, the full-coarsening procedure failed entirely, while the semicoarsening procedure was shown to work very efficiently. It is expected that this modified technique will be an important factor in the multigrid solution of other high Reynolds number flows that display similar sensitivity to normal grid spacing. For these cases, full-coarsening MG is not an effective convergence accelerator.

Convergence rates also were examined for the inviscid subsonic and transonic flows past a parabolic-arc airfoil. The multigrid convergence was found to be much faster than the single-grid convergence. This was found to be the case although the transonic solutions contained gradient singularities (shock waves). It was not necessary to modify the relaxation operator to improve smoothing properties. The multigrid convergence rate was found to improve as the Mach number increased.

### Acknowledgments

This research was supported in part by the Office of Naval Research, through Contract N0014-79-C-0849, and in

part by the Air Force Office of Scientific Research, through Contract F49620-85-C-0027. This paper is dedicated to the first author's mentor Professor William R. Sears on the occasion of his 75th birthday.

### References

- <sup>1</sup>Brandt, A., "Multi-level Adaptive Solutions to Boundary-Value Problems," *Mathematics of Computation*, Vol. 31, 1977, pp. 333-390.
- <sup>2</sup>Brandt, A., "Guide to Multigrid Development," *Proceedings of the Conference on Multigrid Methods*, Springer-Verlag, Berlin, 1981, pp. 220-312.
- <sup>3</sup>Israeli, M., and Lin, A., "Iterative Numerical Solutions and Boundary Conditions for the Parabolized Navier-Stokes Equations," *Proceedings of the 8th ICNMF*, Springer-Verlag, Berlin, 1982, pp. 266-272.
- <sup>4</sup>Israeli, M. and Rosenfeld, M., "Numerical Solution of Incompressible Flows by a Marching Multigrid Nonlinear Method," AIAA Paper 85-1500, 1985.
- <sup>5</sup>Khosla, P.K. and Lai, H.T., "Global PNS Solutions for Subsonic Strong Interaction Flow Over a Cone-Cylinder-Boattail Configuration," *Computers and Fluids*, Vol. 11, No. 4, 1983, pp. 325-340.
- <sup>6</sup>Khosla, P.K. and Lai, H.T., "Global PNS Solutions for Transonic Strong Interaction Flows," AIAA Paper 84-0458, Jan. 1984.
- <sup>7</sup>Lai, H.T., "Global Pressure Relaxation Procedure with Application to Viscous and Inviscid Flows," Ph.D. Dissertation, Dept. of Aerospace Engineering and Engineering Mechanics, Univ. of Cincinnati, Cincinnati, OH, 1985.
- <sup>8</sup>Ramakrishnan, S.V. and Rubin, S.G., "Global Pressure Relaxation for Compressible Flows with Full Pressure Coupling and Shock Waves," Univ. of Cincinnati, Cincinnati, OH, Rept. AFL-85-100, 1984.
- <sup>9</sup>Reddy, D.R., "Global Pressure Relaxation Procedure for Laminar and Turbulent Incompressible Flows with Strong Interaction and Separation," Ph.D. Dissertation, Dept. of Aerospace Engineering and Engineering Mechanics, Univ. of Cincinnati, Cincinnati, OH, 1983.
- <sup>10</sup>Reddy, D.R. and Rubin, S.G., "Subsonic/Transonic, Viscous/Inviscid Relaxation Procedures for Strong Pressure Interactions," AIAA Paper 84-1627, June 1984.
- <sup>11</sup>Rubin, S.G. and Reddy, D.R., "Analysis of Global Pressure Relaxation for Flows with Strong Interaction and Separation," *Computers and Fluids*, Vol. 11, No. 4, 1983, pp. 281-306.
- <sup>12</sup>Stewartson, K., "Multistructured Boundary Layers on Flat Plates and Related Bodies," *Advances in Applied Mechanics*, Vol. 14, Academic, New York, 1974, pp. 145-239.
- <sup>13</sup>Stuben, K. and Trottenberg, U., "Multigrid Methods—Fundamental Algorithms, Model Problem Analysis and Applications," *Proceedings of the Conference on Multigrid Methods*, Springer-Verlag, Berlin, 1981, pp. 1-176.
- <sup>14</sup>Vigneron, Y.C., Rakich, J.V., and Tannehill, J.C., "Calculation of Supersonic Viscous Flow Over Delta Wings with Sharp Subsonic Leading Edges," AIAA Paper 78-1137, July 1978.
- <sup>15</sup>Carter, J.E. and Wornom, S.F., "Solutions for Incompressible Separated Boundary Layers Including Viscous-Inviscid Interaction," NASA SP-347, March 1975.
- <sup>16</sup>Bender, E.E. and Khosla, P.K., "Application of Sparse Matrix Solvers and Newton's Method to Fluid Flow Problems," AIAA Paper 88-3701, July 1988.